Heterogeneous Nucleation in Martensitic Transformations

Turab Lookman and Avadh Saxena, T-11; and Rajeev Ahluwalia, Institute for Materials Research and Engineering, Singapore

Martensites and shape-memory alloys such as certain UNb alloys exhibit unusual mechanical properties due to a diffusionless structural phase transformation from a high temperature (Austenite), in general a cubic, phase to a low temperature (Martensite) tetragonal, orthorhombic or monoclinic phase. This first-order transition is accompanied by a spontaneous strain. The martensitic transition is also responsible for the shape-memory effect that refers to the recovery by heating of an apparently permanent deformation undergone below a critical temperature. This property renders shape-memory materials suitable for a large number of technological and strategic applications. Another important property of shape-memory materials is the so-called pseudoelastic behavior which arises due to a reversible stress/strain-induced martensitic transformation at a temperature that is higher than the austenite finish temperature of the material. In pseudoelastic deformation, a high-temperature cubic austenite phase typically transforms to the martensite under deformation so that there is a plateau in the stress-strain curves. On removing the deformation, the material transforms back to the cubic austenite and the deformation is recovered upon unloading.

Typically, the martensitic transformation results in the formation of a complex microstructure consisting of twin boundaries between the crystallographic variants of the transformation. This microstructure influences the effective mechanical properties of these materials. The motion of the domain walls can influence the strain-rate dependence of the mechanical response. We have theoretically studied the role of microstructural evolution on the mechanical response of shape-memory materials [1], in particular the effects of defect-induced heterogeneous nucleation and motion of twin boundaries during (a representative) cubic to tetragonal deformation of martensite. We have used a displacement field based on a dynamical model to study the effect of defects and microstructure on the stress-strain properties of shape-memory materials. We have also investigated how microstructural evolution influences the strain-rate dependence of the mechanical response.

We present three-dimensional simulations of the microstructure and mechanical response of shape memory alloys undergoing cubic to tetragonal transitions. The dynamics is simulated by force balance equations for the displacement fields with a damping term derived from a dissipation function. Stress-strain properties are investigated using strain loading. To illustrate this, we obtained through a Ginzburg-Landau simulation the stress-strain curves in the presence of defects. The defects will nucleate the transformation

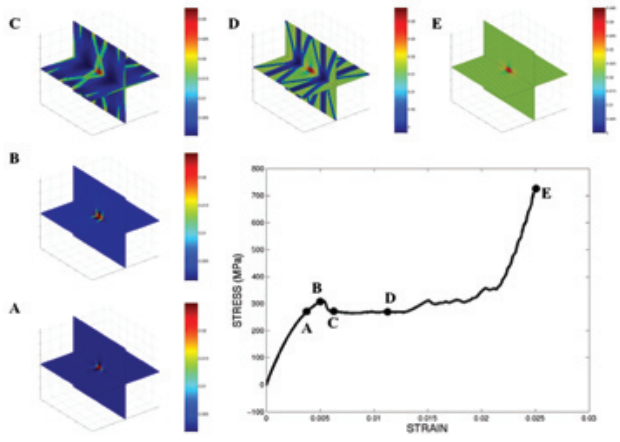

Fig. 1.
Microstructural evolution during uniaxial loading along the x-direction for an embedded tetragonal defect at the center of the cubical simulation box. The various snapshots show the distribution of the strain along the loading direction.

even before the system is in the unstable region, thereby reducing the stress required to cause the transition. We simulated the loading process with an initial "quenched" seed of the transformed phase that is embedded in the initial austenite matrix. The total uniaxial strain field in this direction is given by

$$\varepsilon_{xx} = \partial u_x / \partial_x + \varepsilon \frac{applied}{xx} + \varepsilon \frac{seed}{xx}$$

where $\varepsilon \frac{seed}{xx}$

is the strain due to the defect. This represents an inclusion of a cube of the martensite phase of length L_0 in the austenite matrix.

A loading process for this system with strain rate $\dot{\gamma} = 2.23 \times 10^6/\text{s}$ ($L_0 \sim 24$ nm) is shown in Fig. 1. It shows the stress-strain curve and the spatial distribution of ε_{xx} at points A, B, C, D, and E on the stress-strain curve. To show the evolution of the microstructure, we have displayed two intersecting perpendicular planes that pass through the defect. There is a point on the stress-strain curve where austenite and martensite have the same energy. For strains higher than this critical strain, the nucleation of martensite can take place as martensite has lower energy than the austenite. This nucleation process can be observed by comparing the microstructure at points B and C. One can see the growth of the martensite domains (red) from a seed defect that is embedded in the austenite matrix (blue). On further loading, the favored variant grows, as can be observed in the snapshot corresponding to D. Eventually, a single variant state of the variant stretched along the x direction is established as can be observed in the snapshot E. To test the strain-rate dependence of the stress-strain response in the presence of the defect, Fig. 2 compares the behavior for strain rates $\dot{\gamma} = 8.92 \times 10^6/\text{s}$, $\dot{\gamma} = 4.46 \times 10^6/\text{s}$ and $\dot{\gamma} = 2.23 \times 10^6/\text{s}$ with the analytical solution for the defect-free case. The slower the rate of loading, the smaller is the strain at which the stress deviates from the analytical curve. This is due to the fact that nucleation is not instantaneous and so the time dependence of the nucleation influences the stress-strain response; e.g., if the loading rate is fast enough that there is little time for the martensite to nucleate, the apparent stress required to cause the transition will be higher and the jump at the onset of the transition will be larger. Thus, the jump in stress becomes less pronounced as the strain rate becomes smaller. These results show how nucleation and growth of variants crucially influence the mechanical response in the pseudoelastic regime. Our simulations describe processes at relatively small length (submicron) and time (nanoseconds) scales. Refinement of our scheme to a more coarse-grained model (with volume fractions) is a possible approach to describing larger length scales.

For more information contact Turab Lookman at txl@lanl.gov.

[1] R. Ahluwalia, T. Lookman, and A. Saxena, *Acta Mater.* **54**, (2006).

Funding Acknowledgements
NNSA's Advanced Simulation and Computing (ASC), Materials and Physics Program.

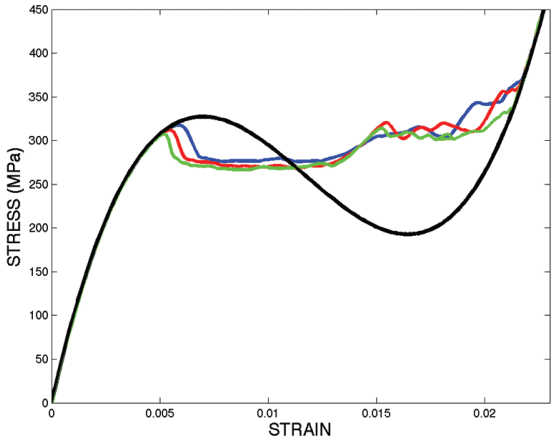

Fig. 2.
Simulated stress-strain curves for the system with a defect for three different strain rates. The black curve represents the homogeneous curve.